BİTLİS EREN ÜNİVERSİTESİ
FEN BİLİMLERİ DERGİSİ

ISSN: 2147-3129 / e-ISSN: 2147-3188

Article Type : Research Article
Received : August 16, 2024
Revised : January 8, 2025
Accepted : January 9, 2025
DOI : 10.17798/bitlisfen.1534686

Year : 2025
Volume : 14
Issue : 1
Pages : 69-87

BIOSORPTION OF OXYTETRACYCLINE FROM AQUEOUS SOLUTIONS BY PINE TREE WASTE CONES *(PINUS NIGRA* ARN.*)*

Talip TURNA [1]

[1] *Dicle University, Department of Parks and Garden Plants, Diyarbakır, Türkiye, talipturna@gmail.com*

ABSTRACT

Removal of Oxytetracycline (OTC), which is in the antibiotic group with toxicological effects for aquatic ecosystems, is very important due to its negative effects on flora and fauna. Adsorption process, which is one of the most effective methods for removing pharmaceutical pollutants, is an economical and environmentally friendly method. For this reason, in this study, biosorbent obtained from pine tree (*Pinus nigra* Arn.) waste cone powder (*Pn*-wcp), which is a low-cost and easily available waste material, was used. The results obtained from the batch adsorption experiments were tested with 4 different kinetic and isotherm models and various error functions were used to determine the most appropriate model. In order to optimize the variables in the adsorption system, contact time and initial OTC concentration factors were investigated. In addition, fourier transform infrared spectroscopy (FTIR), scanning electron microscope (SEM) and energy dispersive X-ray (EDX) images of raw and OTC-loaded *Pn*-wcp were examined. In this study, the most appropriate kinetic model was determined as Pseudo second order (PSO) with 0.999 R^2 value and Freundlich isotherm model with 0.998 R^2 value. In addition, the maximum adsorption capacity (q_{max}) was calculated as 67.51 mgOTC/g*Pn*-wcp. The results show that *Pn*-wcp is a sustainable environmentally friendly biosorbent for OTC removal.

Keywords: Adsorption, Oxytetracycline, Pinus nigra Arn, Kinetics, Isotherm.

1 INTRODUCTION

Antibiotics are used to control bacterial infections in humans and agriculture [1]. With the development of aquaculture and animal husbandry in the world, the use of oxytetracycline (OTC), a type of antibiotic, has increased excessively [2]. Only a small amount of tetracyclines used in treatment can be metabolized or absorbed by humans and animal [3]. Residues of these antibiotics reach the recipient environment and accumulate there, and this accumulation can lead to the emergence of resistant strains with antibiotic resistance [4], [5]. For this reason, antibiotics pose a potential threat to human health through biomagnification and drinking water use [6]. Antibiotics with toxicological properties for flora and fauna are frequently detected in surface waters because conventional wastewater treatment processes cannot adequately remove many of them [7]. Studies have detected OTC as the most abundant antibiotic in two large rivers in the Pearl River System in China, with concentrations of up to 2030 ng/L in water and 2100 ng/g in sediment [8]. The presence of antibiotics that have the potential to reach the recipient environment creates problems due to their possible potential effects on the ecosystem. For these reasons, their elimination is of great importance The development and use of useful water treatment technologies are essential for the removal of these drugs, which have ecotoxicological properties and cause antibiotic resistance in aquatic ecosystems [9] Different removal methods are used for OTC removal from aquatic environments. Various treatment processes such as aerobic systems [10], ozonation [11], electrochemical processes [12], UV degradation [13], adsorption [14], [15] have been frequently applied for OTC removal. Among the alternative methods for OTC removal, the adsorption process is used intensively due to its effectiveness, cheapness, environmental friendliness, and less toxicity [16]. Recently, researchers have been interested in producing low-cost and effective new biosorbents, especially from by-products or waste products obtained from industrial or agricultural processes [17].

In this study, waste pine cones were used to investigate OTC biosorption from aqueous solutions in a batch system. Also 4 different kinetic and isotherm models were tested and various error functions were used to determine the best-fit model. Additionally, pH, contact time and initial OTC concentration factors were investigated to optimize the variables in the adsorption system. Furthermore, FTIR and SEM-EDX images of raw and OTC-loaded pine cone biosorbent were investigated. The results indicate that the biosorbent obtained from waste pine cones is an environmentally sustainable material for OTC removal from aqueous solutions.

2 MATERIAL AND METHOD

2.1 Chemicals

In experimental studies, Pan Trivalent injection solution (Zoetis, Türkiye) was used as OTC source. 1 mL of the solution is equivalent to 30 mg Oxytetracycline hydrochloride. 0.1 M NaOH and 0.1 M H_2SO_4 were used to adjust the pH during the adsorption process.

2.2 Preparation of *Pn-wcp*

The pine cones used in the study were obtained from the area given in the location details (37.910665-40.275318) of Dicle University Campus (Diyarbakır/Türkiye). Pine cones that had fallen under the trees were collected seasonally. The pine cones were first washed with tap water 3 times to remove impurities (mostly leaves and sand), then passed through pure water and dried in sunlight. The dried pine cones were first broken with a pestle and then ground in a laboratory mill. After the process, they were passed through 75-micron sieves and stored for use in experiments.

2.3 Adsorption studies

Adsorption studies were carried out at 25±2 ^{0}C and 200 rpm in an orbital shaker (Heidolp, Unimax1010, Germany). Batch adsorption experiments were carried out in the pH range of 3-10 and especially concentrated at pH 5.0 ±0.5, where OTC has a maximum water solubility [18]. In the wavelength scan, the abs value of the OTC solution with a concentration of 6.6 mg/L and a pH value of 5 was measured as 0.226. The full wavelength scan is presented in Figure 1. OTC stock solution with a concentration of 1000 mg/L was prepared and necessary dilutions were made from the obtained solution to create a calibration curve on a UV-Vis spectrophotometer (Hach DR6000, Germany).

When creating the calibration curve of OTC, necessary dilutions were made from the stock solution. 50 mg/L intermediate stock mixture was obtained, and 2/3 ratios were prepared from 9 different solutions until the ratios reached 2.055 mg/L and the calibration curve was obtained in the spectrophotometer. The equation is $y = 0.0291x + 0.0087$ (R^2:0.999). The absorbance of the OTC solution was carried out with a UV-Vis spectrophotometer at a maximum wavelength of 354 nm to determine the concentration [19]. In a study where OTC removal was performed with activated carbon, it was reported that OTC measurement with UV-Vis peaked in the pH range of 3.68-8.57 and at wavelengths of 354-366 nm [20].

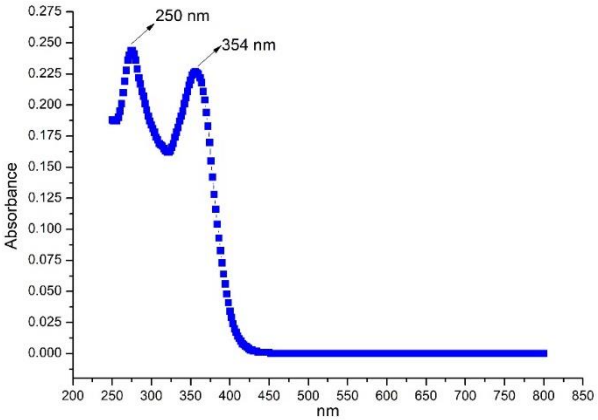

Figure 1. Wavelength scanning results of 6.6 mg/L OTC solution.

MS-Excel program was used in the model calculations of the study and graphics were created with Origin Pro 8.5. Additionally, equations 1 and 2 were used to evaluate the results obtained in each experiment.

$$R(\%) = \frac{C_0 - C_e}{C_0} \times 100 \quad (1)$$

$$q_e = \frac{(C_0 - C_e) \times V}{m} \quad (2)$$

Here, R represents the % removal efficiency, C_0 (mg/L) is the initial OTC concentration, C_e (mg/L) is the equilibrium concentration of OTC, q_e is the equilibrium adsorption capacity, V (L) is the volume of OTC solution, and m (g) is the amount of *Pn*-wcp.

2.4 Impact of environmental factors

The effect of time and initial concentration on the adsorption of OTC molecules onto *Pn*-wcp was tried to be determined. In order to determine the effect of time, 50 mL of OTC solution with an initial concentration of 75 mg/L was taken and 50 mg *Pn*-wcp was added to it. In the experiment carried out at room temperature and pH 5.0 ±0.5, samples were taken at certain time intervals and OTC concentrations were measured. On the other hand, in order to determine the effect of initial OTC concentration on adsorption, OTC solutions were added to 7 different tubes with volumes of 10 mL under the same conditions, with initial concentrations ranging from 10.13 to 116.76 mg/L.

2.5 Kinetic and isotherm studies

For kinetic studies, a 50 mL solution with a concentration of 50 mg/L was prepared from the stock OTC solution. 50 mg of *Pn*-wcp was added to the solution and samples were taken

with a 0.45-micron syringe filter at certain times in the orbital shaker and the concentration was found at the specified wavelengths in the UV-Vis spectrophotometer.

For isotherm studies, experiments were carried out by adding 10 mg of *Pn*-wcp to each of 7 different falcon tubes with a volume of 10 mL, with initial OTC concentrations ranging from 10.13 to 116.76 mg/L. Pseudo first order (PFO), PSO, Intra-particle diffusion and Elovich models were used for kinetic models and interpreted with Freundlich, Langmuir, Temkin and Dubinin-Radushkevich models for isotherm models. The equations used are presented in Table 1.

Table 1. Kinetic and isotherm models used in OTC adsorption on Pn-wcp.

	Model	Equation	References
Kinetic models	PFO	$q_t = q_e(1 - e^{-k_1 t})$	[21]
	PSO	$q_t = \frac{q_e^2 k_2 t}{1 + q_e k_2 t}$	[21]
	Intra-particle diffusion	$q_t = K_{id} t^{1/2} + C$	[22]
	Elovich	$q_t = \beta \ln(\alpha\beta t)$	[22]
Isotherm models	Freundlich	$q_e = K_F {C_e}^{1/n}$	[23]
	Langmuir	$q_e = \frac{q_{max} K_L C_e}{1 + K_L C_e}$ $R_L = \frac{1}{1 + a_L C_e}$	[23]
	Temkin	$q_e = B ln(A_T C_e)$ $B = \frac{RT}{b_T}$	[24]
	Dubinin-Radushkevich	$q_e = q_s e^{-k_D \varepsilon^2}$	[24]

The terms q_t and q_e specified in the table indicate the amount of OTC removed per unit *Pn*-wcp (mg/g) at a time t and under equilibrium, respectively. The term k_1 (min^{-1}) indicates the PFO, the term k_2 (g/mg.min) indicates the PSO and K_{id} indicates the Intra-particle diffusion model constant. α (mg/g.min) indicates the Elovich initial adsorption rate and the term β (g/mg) indicates the desorption constant. In the section where isotherm models are explained, q_e (mg/g) indicates the amount of OTC adsorbed at equilibrium, C_e (mg/L) indicates the OTC concentration at equilibrium and q_{max} (mg/g) indicates the maximum adsorption capacity. K_f (mg/g) (L/mg) is the Freundlich constant *1/n*, *n* is the dimensionless constant and indicates the adsorption density. The terms K_L (L/mg) and a_L are the Langmuir constant. R_L represents the dispersion constant. In addition, *B* in the Temkin model represents the model constant, b_T

(J/mol) represents the heat of adsorption, T (K) represents the temperature, and R (8.314 J/molK) represents the universal gas constant. In the Dubinin-Radushkevich isotherm model, ε represents the Polanyi potential, and k_D represents the model constant.

2.6 Error functions

The use of error functions is extremely important in the evaluation of the adsorption process. Different error functions are usually used to minimize the error distribution between the adsorption experimental data and the isotherm correlations. In order to minimize the error distribution, it is achieved by finding the minimum value of certain error functions or by maximizing them, depending on the definition of the error function used. For this reason, it is very important to choose an error function in order to evaluate the most suitable isotherm that best explains the experimental equilibrium data [25]. The error functions and equations used in the study are presented in Table 2.

Table 2. The error functions and equations used in the study.

Function Definition	Equation	References
Error Sum of Squares (*SSE*)	$SSE = \sum (q_{e,cal} - q_{e,exp})^2$	[26], [27]
Sum of Absolute Errors (*SAE*)	$SAE = \sum_{i=1}^{n} \left\|q_{e,exp} - q_{e,cal}\right\|$	
Average relative errors (*ARE*)	$RAE = \frac{1}{n}\sum_{i=1}^{n} \left\|\frac{q_{e,cal} - q_{e,exp}}{q_{e,exp}}\right\|$	
Hybrid fractional error function (*HYBRID*)	$\text{HYBRID} = \frac{1}{N-P}\sum \left\|\frac{q_{e,exp} - q_{e,cal}}{q_{e,exp}}\right\|$	[27]
Marquardt's percent standard deviation (*MPSD*)	$MPSD = \sqrt{\frac{\sum\left\|(q_{e,exp} - q_{e,cal})/q_{e,exp}\right\|^2}{N-P}}$	[26]
Non-linear Chi-Square test (X^2)	$X^2 = \sum \frac{(q_{e,exp} - q_{e,cal})^2}{q_{e,cal}}$	[26], [27]

In order to evaluate the adsorption results, different error function models were used to examine the kinetic models. Five error analysis methods were used to determine the kinetic model parameters in the study. These are Sum of Absolute Error (*SAE*), Marquart's percent standard deviation (*MPSD*), sum of squared errors (*SSE*), hybrid fractional error function (*HYBRID*), mean relative error (*ARE*) and Nonlinear Chi-Square (X^2) error functions.

3 RESULTS AND DISCUSSION

3.1 Characterization results

3.1.1 FTIR results

FTIR spectra of raw *Pn*-wcp before the reaction and OTC-loaded *Pn*-wcp after the reaction are presented in Figure 2. Functional groups are seen between both cases.

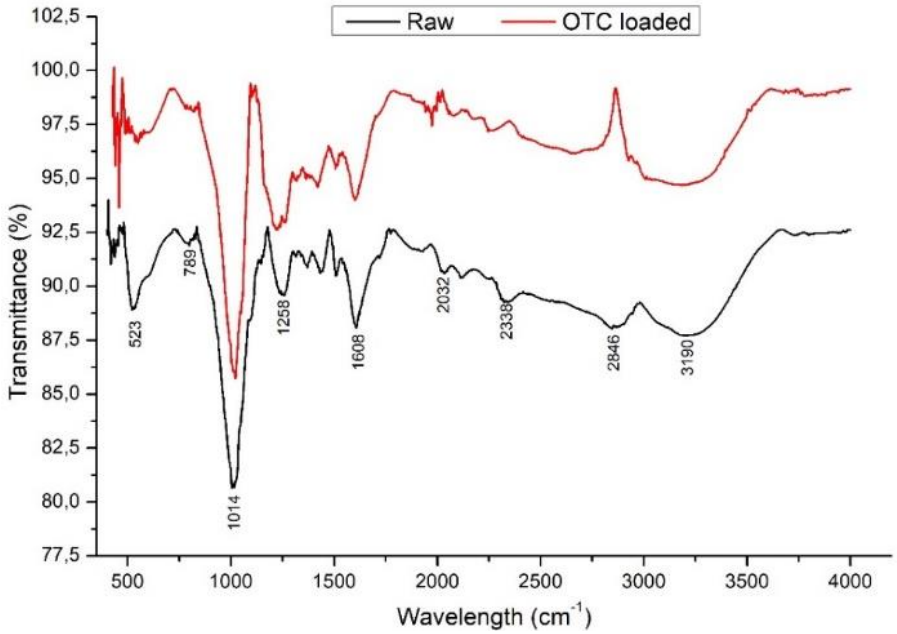

Figure 2. FTIR diagram of Pn-wcp before and after reaction.

In the spectrum of the raw adsorbent, characteristic absorption bands are observed at wavelengths of 523 cm^{-1}, 789 cm^{-1}, 1014 cm^{-1}, 1258 cm^{-1}, 1608 cm^{-1}, 2032 cm^{-1}, 2338 cm^{-1}, 2846 cm^{-1} and 3190 cm^{-1}. These bands indicate the presence of functional groups (such as hydroxyl, carbonyl, and carboxyl groups) on the surface of the adsorbent. Especially the bands around 1608 cm^{-1} indicate the C-O and C=C stretching, and therefore the presence of lignin, cellulose, and other organic components [28].

Aliphatic C–H stretching vibration is found as a very weak peak at 2846 cm^{-1}, while the asymmetric vibration of CH_2 group belonging to aliphatic cellulose vibration is seen at 3190 cm^{-1} [29], [30]. The bands between 523 and 1014 cm^{-1} represent –C–N– and –C–C– stretching, respectively [31]. After OTC adsorption, the obvious changes in the spectrum indicate that there is a chemical interaction on the surface of the adsorbent. Especially, the obvious changes in the regions of 1258 cm^{-1}, 1608 cm^{-1} and 2846 cm^{-1} may indicate that OTC interacts with the adsorbent surface and is probably held by hydrogen bonds or Van der Waals forces.

3.1.2 SEM and EDX results

The SEM imaging technique is an important tool for characterizing active sorptive surface areas and basic physical properties of biosorbent surfaces. It helps in morphological characterization by providing information about particle shape and size distribution. The surface morphology of *Pn*-wcp was imaged before and after adsorption and is presented in Figure 3. When Figure 3-a is examined, it is seen that *Pn*-wcp exhibits a rough, irregular, heterogeneous structure. This structure creates the necessary areas for the biosorption of OTC. In the image obtained after adsorption (Figure 3-b), the pores are partially filled, and the roughness is reduced.

The possible reason for this situation is that OTC molecules are adsorbed on the surface and pores. When the EDX graphs given in Figure 3 are examined, the changes after adsorption and the differences in element ratios support the successful adsorption of OTC molecules [32]. It can be said that especially oxygen groups play an active role in the process and are connected to the surface with the carbon-based structure of OTC.

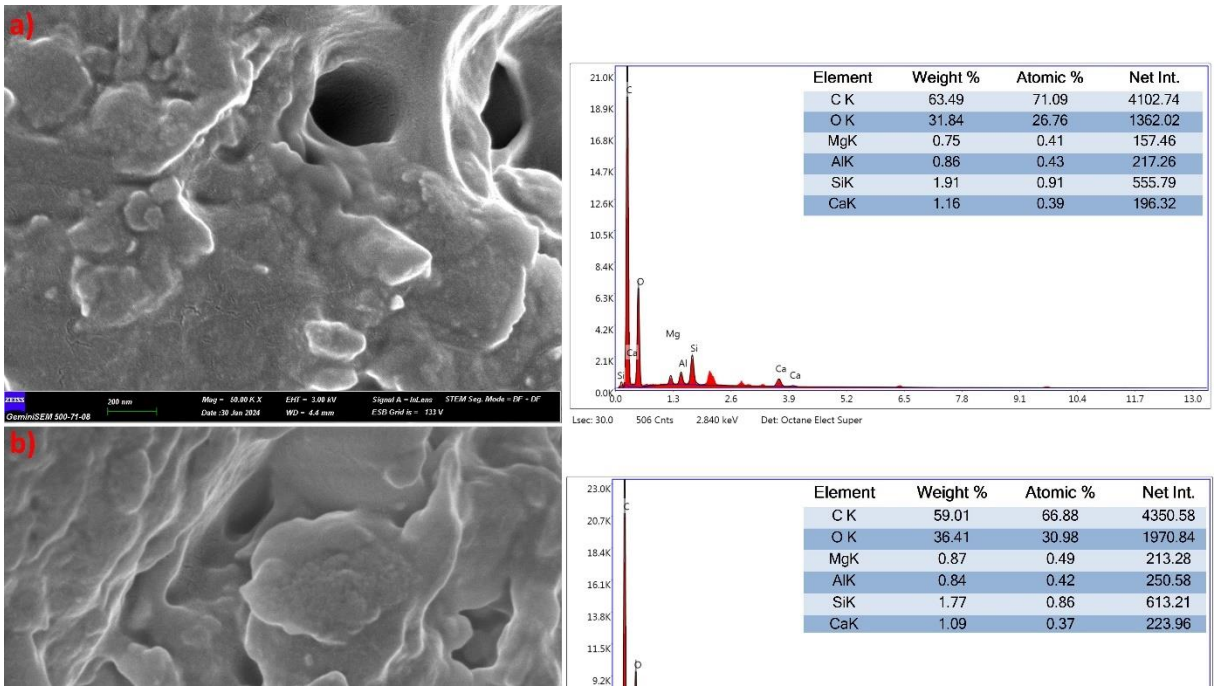

Figure 3. (a) SEM and EDX images of Pn-wcp before (b) and after reaction.

3.2 Adsorption Results

3.2.1 Effect of contact time on removal efficiency

The results obtained from the studies conducted to determine the effect of time on the adsorption of OTC molecules onto *Pn*-wcp particles are presented in Figure 4.

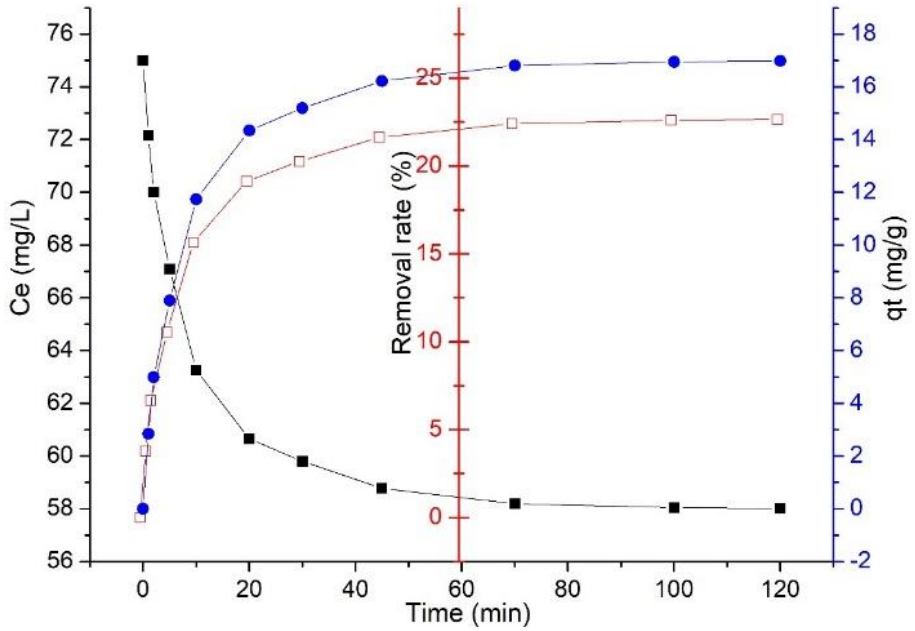

Figure 4. Effect of time on the adsorption of OTC molecules onto Pn-wcp particles.

According to Figure 4, the removal efficiency in the 1st minute was 3.8%, while it reached 10.5% in the 5th minute and 21.6% in the 45th minute, and the efficiency increase decreased in the following minutes. When the *qt* values were examined, it was determined as 2.85 mg/g in the 1st minute, 7.90 mg/g in the 5th minute and 16.22 mg/g in the 45th minute. Similarly, the increase rate slows down considerably in the following minutes. Accordingly, the removal efficiency increases with the increase in the contact time of OTC particles and OTC molecules on *Pn*-wcp. The results showed that there was a rapid adsorption in the first minutes, then it gradually increased with increasing contact time until equilibrium was reached. When Figure 4 is examined, the gradual increase that started rapidly slowed down for a certain period and then reached equilibrium. The probable reason for this is that the sorption areas become close to saturation [33].

3.2.2 Effect of initial concentration on removal efficiency

The results obtained from the experiments conducted to determine the effect of initial OTC concentration on the adsorption of OTC molecules onto *Pn*-wcp particles are presented in Figure 5.

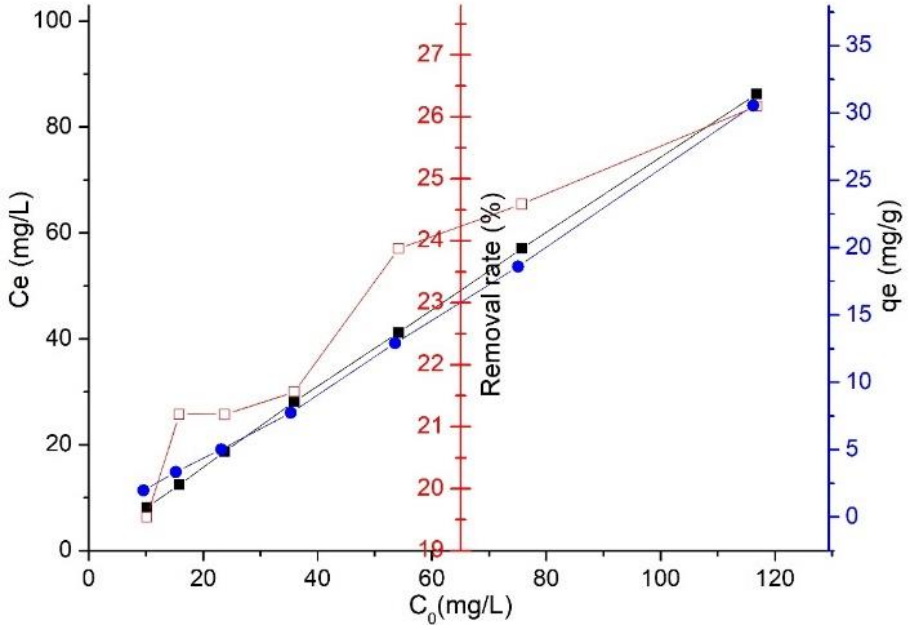

Figure 5. Effect of initial OTC concentration on the adsorption of OTC molecules onto Pn-wcp particles.

When Figure 5 is examined, when the initial OTC concentration is 10.13 mg/L, the removal efficiency is calculated as 19.55%, when the OTC concentration reaches 35.90 mg/L, the efficiency reaches 21.56%, and when the initial OTC concentration is 116.76 mg/L, the efficiency is calculated as 26.17%. When the removal efficiencies per unit adsorbent are examined, the initial OTC concentrations are calculated as 1.98, 7.74 and 30.56 mg/g at 10.16, 35.90 and 116.76 mg/L, respectively. Accordingly, the increase in the OTC change in the medium causes an increase in the adsorption capacity in the removal efficiency. When the literature is examined, it was reported that the removal efficiency increased with the increase in OTC concentration in the adsorption study of OTC hydrochloride on magnetic zeolite/Fe_3O_4 particles[34].

3.2.3 Adsorption kinetics

Adsorption kinetic models are very important for evaluating the performance of the adsorbent and investigating the adsorption mass transfer mechanisms [35]. In this study, the results obtained from 4 different kinetic models were compared with each other and presented in Table 3. In addition, the graphs obtained from the linearized forms of each model equation are also presented in Figure 6. The numerical values obtained in the laboratory environment during the adsorption of OTC molecules by *Pn*-wcp particles were tested with PFO, PSO, Elovich and Intra-particle diffusion models, respectively. In addition to these, the change graph comparing the numerical values obtained from the applied kinetic models with the amount of pollutant removed by the unit adsorbent (q_t) obtained in the experimental studies is given in Figure 7.

Table 3. Summary of the calculated kinetic models for the adsorption of OTC onto Pn-wcp.

Kinetic models	**PFO**	**PSO**	**Elovich**	**Intra-Particle Diffusion**
Parameters	$k_1 = 0.052$	$k_2 = 0.011$	$\beta = 0.317$	$k_i = 1.321$
		$q_e = 17.834$	$\alpha = 9.377$	$a = 5.295$
R^2	0.987	0.999	0.958	0.784
SSE	50.704	0.875	9.432	55.758
SAE	16.810	1.665	8.719	21.222
ARE	33.70	2.47	12.38	39.94
HYBRID	47.184	1.614	4.942	26.204
MPSD	0.993	0.960	0.970	0.987
X^2	6.746	0.102	0.797	8.394

When Table 3 is examined, the R^2 values of the PFO, Elovich and Intra-particle diffusion models were calculated as 0.987-0.958 and 0.784, respectively, while the R^2 value of the PSO model was calculated as 0.999. The evaluation of error functions in the selection of the most appropriate model is very important in terms of the accuracy of the result. The lower the error value obtained in the model, the better the performance of the estimated model [36]. When the *SSE* value, which is the sum of the squares of the difference between the amounts of pollutants removed per unit adsorbent ($q_{e,cal}$) obtained from the examined kinetic models and the results obtained from the adsorption process ($q_{e,exp}$), is examined, it is seen that the PSO kinetic model has the smallest value (0.875). Again, in the *SAE* value, which is the sum of the absolute value of the difference between the batch adsorption experimental results and the model results, the PSO kinetic model is the lowest with the value of (1.665).

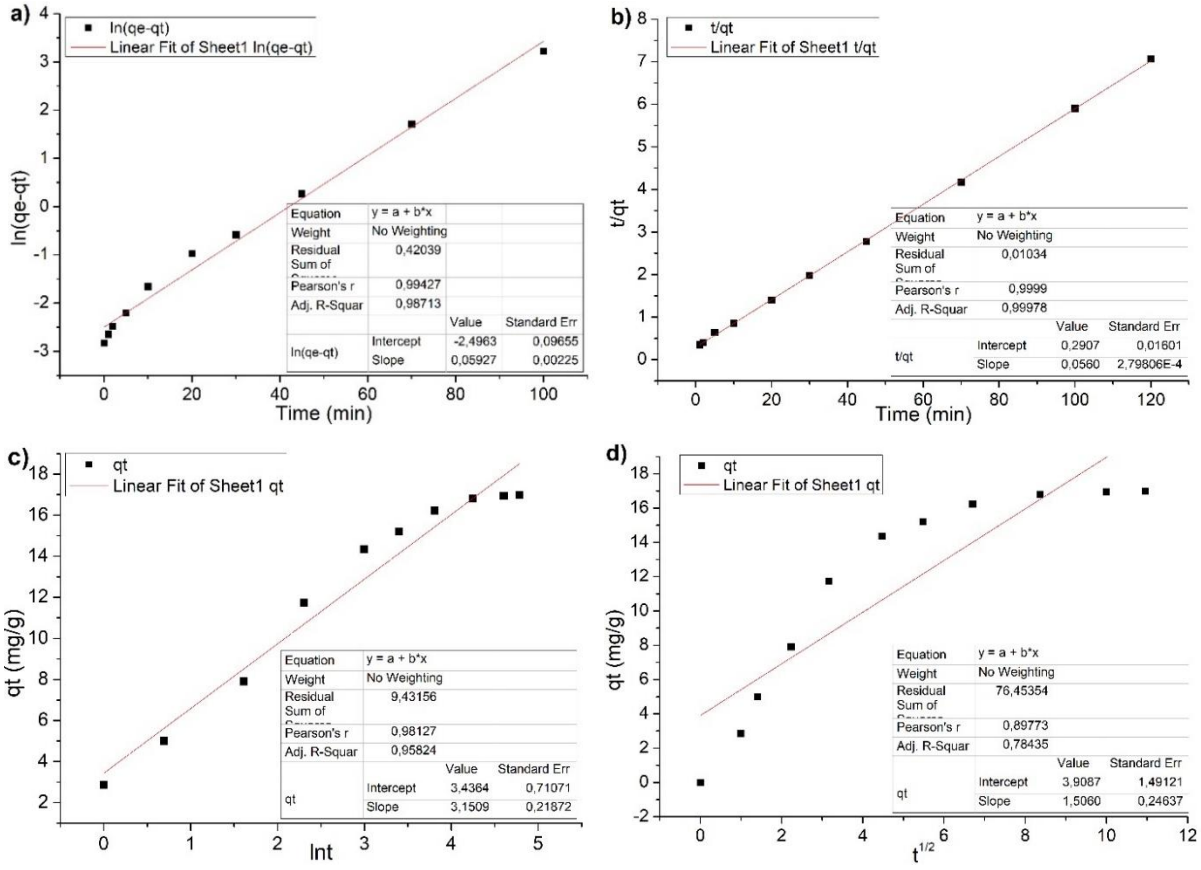

Figure 6. Regression curves, a) PFO, b) PSO, c) Elovich, d) Intra-Particle Diffusion.

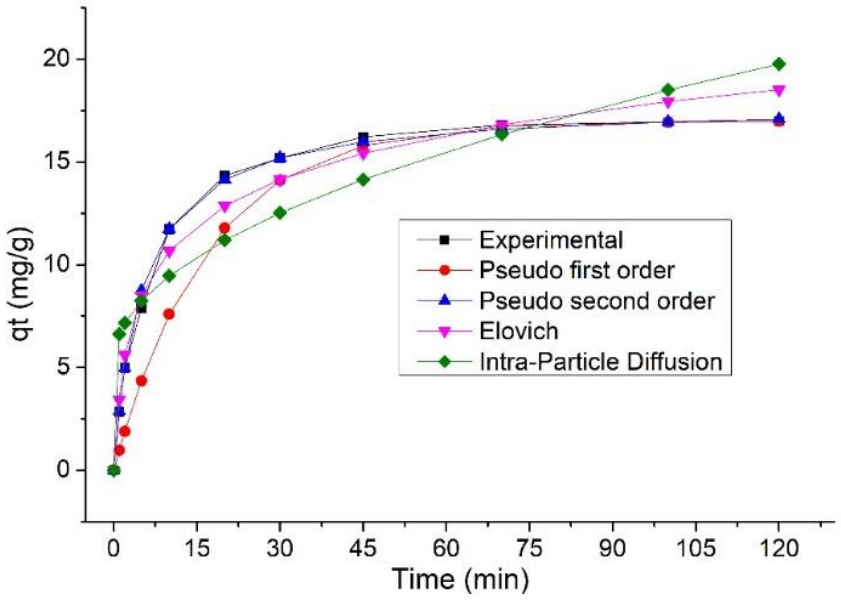

Figure 7. Graph of q_t values versus time.

When the *ARE* value obtained from the absolute value of the difference between the model and adsorption experiments divided by the experimental results is examined, it is understood that the PSO kinetic model is the lowest with the value of (2.47). In the *HYBRID* value obtained as a result of the $q_{e,cal}$ division of the *SSE* values, the lowest value is again in the PSO model with the value of (1.614) and in the *MPSD* value, which is the error calculation made regarding the geometric error distribution, (0.960).

When different literature studies were examined, it was stated that the PSO kinetic model was the model that best explained the process with the value of R^2: 0.999 in the study on OTC adsorption using pine cone biochar modified with MnO_2 [32]. Similarly, in the study on the removal of tetracycline from water with activator agents using activated carbon obtained from pine cones, it was reported that the PSO model was the model that best explained the adsorption process with the value of R^2: 0.994 [38]. In a different study, it was stated that the removal of tetracycline with pine cone biochar prepared by hydrothermal pretreatment with KOH solution was aimed, and the adsorption process was similarly suitable for the PSO model [39]. When the obtained R^2 values and error functions were evaluated together, it was seen that the PSO kinetic model was the most suitable model to explain the process among these 4 models.

3.2.4 Adsorption isotherms

The application of adsorption isotherms is very important to explain the interaction between the adsorbate and the adsorbent of any system. The parameters obtained from the modeling of isotherm results provide important information for the appropriate analysis and design of the adsorption system [40]. In this study, Freundlich, Langmuir, Temkin and Dubinin-Radushkevich isotherm models were used to interpret the data obtained from the experiments conducted for the adsorption of OTC molecules onto *Pn*-wcp particles. The results obtained from the models are presented in Table 4. In addition, the graphs obtained from the linear forms of each model are presented in Figure 8 (a), (b) (c) and (d). In addition, the comparison graph of *qt* values against C_e values, in which the isotherm models used are compared, is given in Figure 9.

Table 4. Summary of isotherm models calculated for the adsorption of OTC molecules onto Pn-wcp.

Isotherms	Freundlich	Langmuir	Temkin	Dubinin-Radushkevich
Parameters	k_F = 0.176	k_L = 0.004	B_T = 0.216	k_D = 29.041
	$1/n$ = 1.153	R_L = 0.8	k_T = 0.102	q_s = 14.354
		q_{max} = 67.512		E = 0.131
R^2	0.998	0.917	0.831	0.682
SSE	0.752	266.363	88.122	332.334
SAE	1.605	27.367	21.668	31.770
ARE	3.3	31.1	75.1	58.3
HYBRID	0.07	31.07	23.34	14.74
MPSD	0.930	0.988	0.986	0.981
X^2	0.056	10.681	13.846	16.446

When Table 4 is examined, the R^2 values of the Langmuir, Temkin and Dubinin-Radushkevich models were calculated as (0.917), (0.831) and (0.682), respectively, while the R^2 value of the Freundlich model was found to be 0.998. In the evaluation made with error functions, when the *SSE, SAE, ARE, HYBRID, MPSD* and X^2 values were examined, they were calculated as (0.752), (1.605), (3.3), (0.07), (0.930) and (0.056), respectively. When similar literature studies were examined, the isotherm model in the study on the adsorption of quinolone antibiotics in water with activated carbon was defined as the Freundlich isotherm [41]. In the study carried out by Alnajrani and Alsager for the removal of antibiotics from aqueous environments, they reported that the Freundlich model with the highest R^2 values represented the process in the best way [42]. As a result, when both R^2 values and error functions are evaluated together in our study, it is seen that the adsorption of OTC molecules on *Pn*-wcp particles conforms to the Freundlich isotherm model.

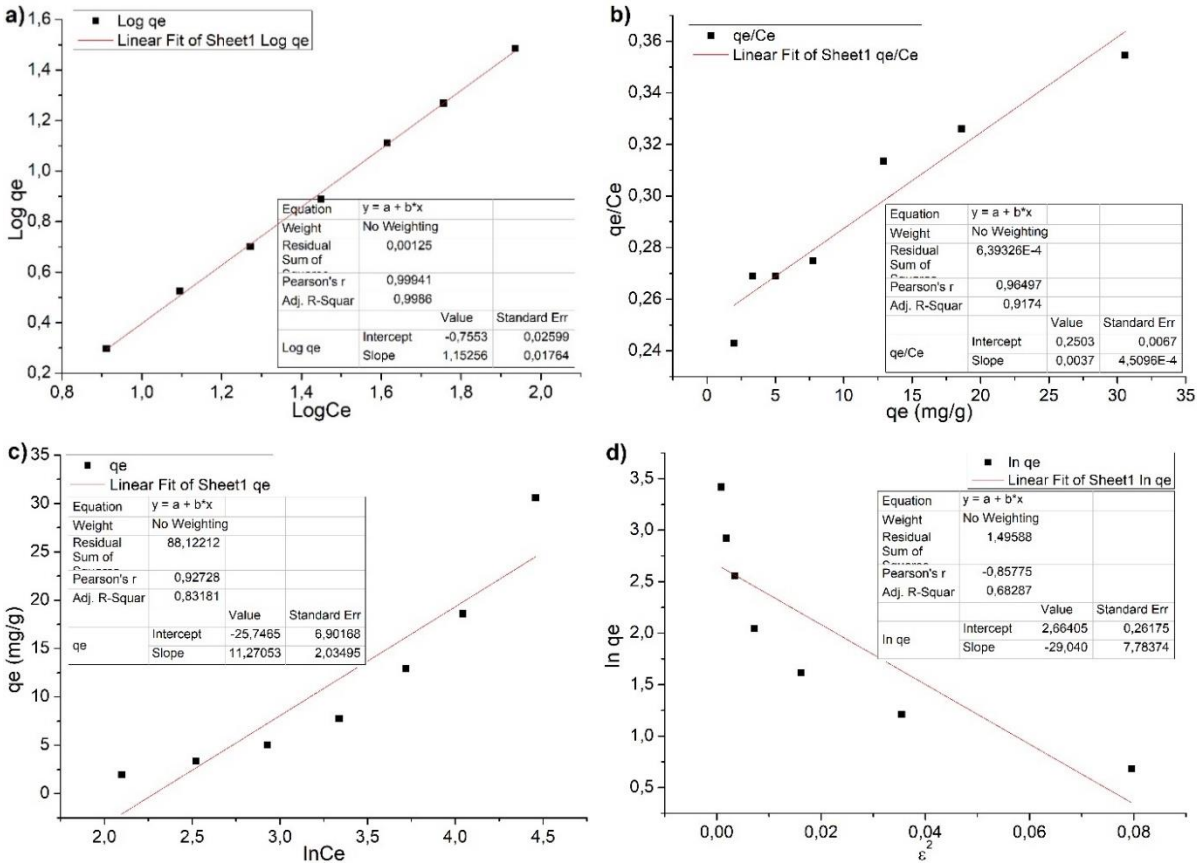

Figure 8. Regression curves (a) Freundlich, b) Langmuir, c) Temkin, d) Dubinin – Radushkevich.

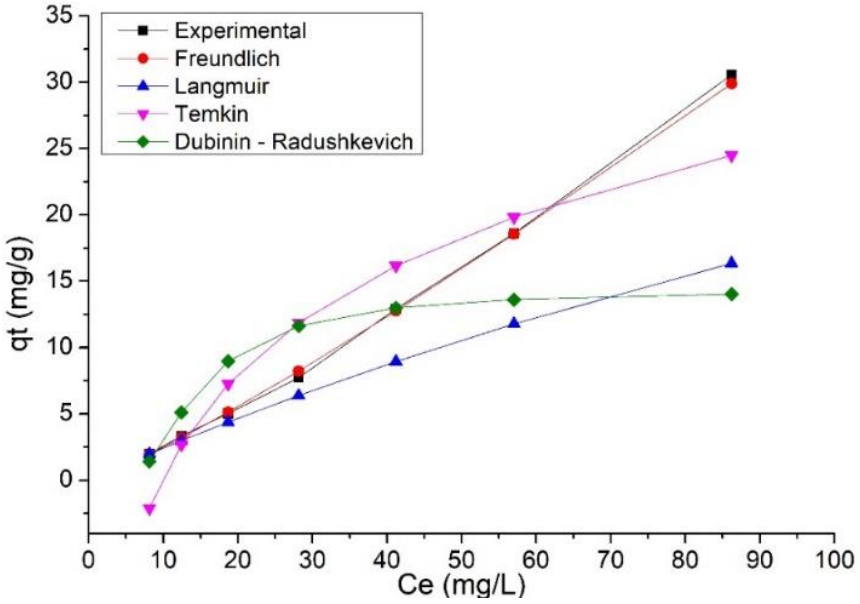

Figure 9. Graph of change of qt values against C_e values.

3.2.5 Comparison of the study and the results obtained with the literature.

When the studies in the literature (Table 5) are examined, the maximum adsorption capacity was determined as 90.9 mg/g in a study where OTC was removed from an aqueous solution with activated sludge. The maximum adsorption capacity was determined as 598 mg/g in a study where OTC was removed with activated carbon obtained from mesoporous lignin.

Table 5. Comparison of the obtained values with the literature.

Type of pollutant	Adsorbent origin	q_m (mg/g)	Reference
OTC	Activated sludge	90.9	[43]
OTC	Lignin-based carbon with mesoporous	598	[44]
OTC	Lanthanum modified magnetic humic acid	23.43	[45]
OTC	Hydroxyapatite	291.32	[33]
OTC	*Pn*-wcps	67.51	This study

The maximum adsorption capacity was determined as 23.43 mg/g in a similar study where OTC was removed with lanthanum modified magnetic humic acid. In another adsorption study where OTC was removed from an aqueous solution with hydroxyapatite, the maximum adsorption capacity was reported as 291.32 mg/g. In our study, the maximum adsorption capacity was found as 67.51 mg/g.

4 CONCLUSION AND SUGGESTIONS

In this research study, low-cost biosorbent obtained from waste pine cones was used for OTC removal from aqueous solutions in laboratory scale. 4 different kinetic and isotherm models were investigated in bulk adsorption studies. In addition, FTIR and SEM-EDX images were examined to investigate the morphological properties of raw and loaded *Pn*-wcps to support the adsorption mechanism. In the evaluation of the obtained results together with error tests, the most suitable kinetic and isotherm models were found to be PSO (R^2: 0.999) and Freundlich (R^2: 0.998), respectively. On the other hand, q_{max} was calculated as 67.51 mgOTC/g*Pn*-wcp. When the optimization studies carried out around pH 5.0 ±0.5 were evaluated, it was found that the gradual increase that started rapidly slowed down for a while and then reached equilibrium. In addition, the increase in OTC concentration in the medium caused an increase in removal efficiency and adsorption capacity. This study may be an example of different combination studies that can be applied in the removal of broad-spectrum OTC, which is used very intensively in the world, from aquatic environments in order to reduce the possible harmful effects on the environment after its use.

Statement of Research and Publication Ethics

The study is complied with research and publication ethics.

Artificial Intelligence (AI) Contribution Statement

This manuscript was entirely written, edited, analyzed, and prepared without the assistance of any artificial intelligence (AI) tools. All content, including text, data analysis, and figures, was solely generated by the author.

REFERENCES

[1] R. Ding *et al.*, "Light-excited photoelectrons coupled with bio-photocatalysis enhanced the degradation efficiency of oxytetracycline," *Water Res*, vol. 143, pp. 589–598, Oct. 2018, doi: 10.1016/j.watres.2018.06.068.

[2] Z. LI, W. QI, Y. FENG, Y. LIU, S. Ebrahim, and J. LONG, "Degradation mechanisms of oxytetracycline in the environment," *J Integr Agric*, vol. 18, no. 9, pp. 1953–1960, Sep. 2019, doi: 10.1016/S2095-3119(18)62121-5.

[3] M. Karpov, B. Seiwert, V. Mordehay, T. Reemtsma, T. Polubesova, and B. Chefetz, "Transformation of oxytetracycline by redox-active Fe (III)- and Mn(IV)-containing minerals: Processes and mechanisms," *Water Res*, vol. 145, pp. 136–145, Nov. 2018, doi: 10.1016/j.watres.2018.08.015.

[4] P. Gao, M. Munir, and I. Xagoraraki, "Correlation of tetracycline and sulfonamide antibiotics with corresponding resistance genes and resistant bacteria in a conventional municipal wastewater treatment plant," *Science of The Total Environment*, vol. 421–422, pp. 173–183, Apr. 2012, doi: 10.1016/j.scitotenv.2012.01.061.

[5] H. Schmitt, K. Stoob, G. Hamscher, E. Smit, and W. Seinen, "Tetracyclines and Tetracycline Resistance in Agricultural Soils: Microcosm and Field Studies," *Microb Ecol*, vol. 51, no. 3, pp. 267–276, Apr. 2006, doi: 10.1007/s00248-006-9035-y.

[6] L. M. Chiesa, M. Nobile, S. Panseri, and F. Arioli, "Suitability of feathers as control matrix for antimicrobial treatments detection compared to muscle and liver of broilers," *Food Control*, vol. 91, pp. 268–275, Sep. 2018, doi: 10.1016/j.foodcont.2018.04.002.

[7] P. Gao, Y. Ding, H. Li, and I. Xagoraraki, "Occurrence of pharmaceuticals in a municipal wastewater treatment plant: Mass balance and removal processes," *Chemosphere*, vol. 88, no. 1, pp. 17–24, Jun. 2012, doi: 10.1016/j.chemosphere.2012.02.017.

[8] F.-Z. Gao *et al.*, "The variations of antibiotics and antibiotic resistance genes in two subtropical large river basins of south China: Anthropogenic impacts and environmental risks," *Environmental Pollution*, vol. 312, p. 119978, Nov. 2022, doi: 10.1016/j.envpol.2022.119978.

[9] M. Harja and G. Ciobanu, "Studies on adsorption of oxytetracycline from aqueous solutions onto hydroxyapatite," *Science of The Total Environment*, vol. 628–629, pp. 36–43, Jul. 2018, doi: 10.1016/j.scitotenv.2018.02.027.

[10] X. Wang, J. Shen, J. Kang, X. Zhao, and Z. Chen, "Mechanism of oxytetracycline removal by aerobic granular sludge in SBR," *Water Res*, vol. 161, pp. 308–318, Sep. 2019, doi: 10.1016/j.watres.2019.06.014.

[11] J.-A. Park, M. Pineda, M.-L. Peyot, and V. Yargeau, "Degradation of oxytetracycline and doxycycline by ozonation: Degradation pathways and toxicity assessment," *Science of The Total Environment*, vol. 856, p. 159076, Jan. 2023, doi: 10.1016/j.scitotenv.2022.159076.

[12] W. Sun, Y. Sun, K. J. Shah, H. Zheng, and B. Ma, "Electrochemical degradation of oxytetracycline by Ti-Sn-Sb/γ-Al2O3 three-dimensional electrodes," *J Environ Manage*, vol. 241, pp. 22–31, Jul. 2019, doi: 10.1016/j.jenvman.2019.03.128.

[13] Y. Wang *et al.*, "Schwertmannite catalyze persulfate to remove oxytetracycline from wastewater under solar light or UV-254," *J Clean Prod*, vol. 364, p. 132572, Sep. 2022, doi: 10.1016/j.jclepro.2022.132572.

[14] A. Solmaz, M. Karta, T. Depci, T. Turna, and Z. A. Sari, "Preparation and characterization of activated carbons from Lemon Pulp for oxytetracycline removal," *Environ Monit Assess*, vol. 195, no. 7, p. 797, Jul. 2023, doi: 10.1007/s10661-023-11421-4.

[15] Y. Liu, N. Tan, B. Wang, and Y. Liu, "Stepwise adsorption-oxidation removal of oxytetracycline by Zn0-CNTs-Fe3O4 from aqueous solution," *Chemical Engineering Journal*, vol. 375, p. 121963, Nov. 2019, doi: 10.1016/j.cej.2019.121963.

[16] J. Zhou, F. Ma, H. Guo, and D. Su, "Activate hydrogen peroxide for efficient tetracycline degradation via a facile assembled carbon-based composite: Synergism of powdered activated carbon and ferroferric oxide nanocatalyst," *Appl Catal B*, vol. 269, p. 118784, Jul. 2020, doi: 10.1016/j.apcatb.2020.118784.

[17] M. B. Ahmed, J. L. Zhou, H. H. Ngo, and W. Guo, "Adsorptive removal of antibiotics from water and wastewater: Progress and challenges," *Science of The Total Environment*, vol. 532, pp. 112–126, Nov. 2015, doi: 10.1016/j.scitotenv.2015.05.130.

[18] Z. Li, H. Jiang, X. Wang, C. Wang, and X. Wei, "Effect of pH on Adsorption of Tetracycline Antibiotics on Graphene Oxide," *Int J Environ Res Public Health*, vol. 20, no. 3, p. 2448, Jan. 2023, doi: 10.3390/ijerph20032448.

[19] A. Kumar Subramani, P. Rani, P.-H. Wang, B.-Y. Chen, S. Mohan, and C.-T. Chang, "Performance assessment of the combined treatment for oxytetracycline antibiotics removal by sonocatalysis and degradation using Pseudomonas aeruginosa," *J Environ Chem Eng*, vol. 7, no. 4, p. 103215, Aug. 2019, doi: 10.1016/j.jece.2019.103215.

[20] M. Berger, J. Ford, and J. L. Goldfarb, "Modeling aqueous contaminant removal due to combined hydrolysis and adsorption: oxytetracycline in the presence of biomass-based activated carbons," *Sep Sci Technol*, vol. 54, no. 5, pp. 705–721, Mar. 2019, doi: 10.1080/01496395.2018.1520721.

[21] X. Guo and J. Wang, "A general kinetic model for adsorption: Theoretical analysis and modeling," *J Mol Liq*, vol. 288, p. 111100, Aug. 2019, doi: 10.1016/j.molliq.2019.111100.

[22] J. Wang and X. Guo, "Adsorption kinetic models: Physical meanings, applications, and solving methods," *J Hazard Mater*, vol. 390, p. 122156, May 2020, doi: 10.1016/j.jhazmat.2020.122156.

[23] M. Mozaffari Majd, V. Kordzadeh-Kermani, V. Ghalandari, A. Askari, and M. Sillanpää, "Adsorption isotherm models: A comprehensive and systematic review (2010−2020)," *Science of The Total Environment*, vol. 812, p. 151334, Mar. 2022, doi: 10.1016/j.scitotenv.2021.151334.

[24] J. Wang and X. Guo, "Adsorption isotherm models: Classification, physical meaning, application and solving method," *Chemosphere*, vol. 258, p. 127279, Nov. 2020, doi: 10.1016/j.chemosphere.2020.127279.

[25] S. M. Miraboutalebi, S. K. Nikouzad, M. Peydayesh, N. Allahgholi, L. Vafajoo, and G. McKay, "Methylene blue adsorption via maize silk powder: Kinetic, equilibrium, thermodynamic studies and residual error analysis," *Process Safety and Environmental Protection*, vol. 106, pp. 191–202, Feb. 2017, doi: 10.1016/j.psep.2017.01.010.

[26] H. Alrobei *et al.*, "Adsorption of anionic dye on eco-friendly synthesised reduced graphene oxide anchored with lanthanum aluminate: Isotherms, kinetics and statistical error analysis," *Ceram Int*, vol. 47, no. 7, pp. 10322–10331, Apr. 2021, doi: 10.1016/j.ceramint.2020.07.251.

[27] S. S. A. Alkurdi, R. A. Al-Juboori, J. Bundschuh, L. Bowtell, and A. Marchuk, "Inorganic arsenic species removal from water using bone char: A detailed study on adsorption kinetic and isotherm models using error functions analysis," *J Hazard Mater*, vol. 405, p. 124112, Mar. 2021, doi: 10.1016/j.jhazmat.2020.124112.

[28] I. L. A. Ouma, E. B. Naidoo, and A. E. Ofomaja, "Thermodynamic, kinetic and spectroscopic investigation of arsenite adsorption mechanism on pine cone-magnetite composite," *J Environ Chem Eng*, vol. 6, no. 4, pp. 5409–5419, Aug. 2018, doi: 10.1016/j.jece.2018.08.035.

[29] M. Momčilović, M. Purenović, A. Bojić, A. Zarubica, and M. Ranđelović, "Removal of lead(II) ions from aqueous solutions by adsorption onto pine cone activated carbon," *Desalination*, vol. 276, no. 1–3, pp. 53–59, Aug. 2011, doi: 10.1016/j.desal.2011.03.013.

[30] N. S. Kumar, M. Asif, and M. I. Al-Hazzaa, "Adsorptive removal of phenolic compounds from aqueous solutions using pine cone biomass: kinetics and equilibrium studies," *Environmental Science and Pollution Research*, vol. 25, no. 22, pp. 21949–21960, Aug. 2018, doi: 10.1007/s11356-018-2315-5.

[31] E. Malkoc, "Ni(II) removal from aqueous solutions using cone biomass of Thuja orientalis," *J Hazard Mater*, vol. 137, no. 2, pp. 899–908, Sep. 2006, doi: 10.1016/j.jhazmat.2006.03.004.

[32] R. Zafar *et al.*, "Efficient and simultaneous removal of four antibiotics with silicone polymer adsorbent from aqueous solution," *Emerg Contam*, vol. 9, no. 4, p. 100258, Dec. 2023, doi: 10.1016/j.emcon.2023.100258.

[33] M. Harja and G. Ciobanu, "Studies on adsorption of oxytetracycline from aqueous solutions onto hydroxyapatite," *Science of The Total Environment*, vol. 628–629, pp. 36–43, Jul. 2018, doi: 10.1016/j.scitotenv.2018.02.027.

[34] G. Başkan, Ü. Açıkel, and M. Levent, "Investigation of adsorption properties of oxytetracycline hydrochloride on magnetic zeolite/Fe3O4 particles," *Advanced Powder Technology*, vol. 33, no. 6, p. 103600, Jun. 2022, doi: 10.1016/j.apt.2022.103600.

[35] J. Wang and X. Guo, "Adsorption kinetic models: Physical meanings, applications, and solving methods," *J Hazard Mater*, vol. 390, p. 122156, May 2020, doi: 10.1016/j.jhazmat.2020.122156.

[36] A. Terdputtakun, O. Arqueropanyo, P. Sooksamiti, S. Janhom, and W. Naksata, "Adsorption isotherm models and error analysis for single and binary adsorption of Cd(II) and Zn(II) using leonardite as adsorbent," *Environ Earth Sci*, vol. 76, no. 22, p. 777, Nov. 2017, doi: 10.1007/s12665-017-7110-y.

[37] P. Bobde, A. K. Sharma, R. Kumar, S. Pal, J. K. Pandey, and S. Wadhwa, "Adsorptive removal of oxytetracycline using MnO2-engineered pine-cone biochar: thermodynamic and kinetic investigation and process optimization," *Environ Monit Assess*, vol. 195, no. 11, p. 1291, Nov. 2023, doi: 10.1007/s10661-023-11932-0.

[38] S. O. Sanni, O. Oluokun, S. O. Akpotu, A. Pholosi, and V. E Pakade, "Removal of tetracycline from the aquatic environment using activated carbon: A comparative study of adsorption performance based on the activator agents," *Heliyon*, vol. 10, no. 14, p. e34637, Jul. 2024, doi: 10.1016/j.heliyon.2024.e34637.

[39] S. Wang, L. Wu, L. Wang, J. Zhou, H. Ma, and D. Chen, "Hydrothermal Pretreatment of KOH for the Preparation of PAC and Its Adsorption on TC," *Materials*, vol. 16, no. 14, p. 4966, Jul. 2023, doi: 10.3390/ma16144966.

[40] M. J. Ahmed, "Adsorption of quinolone, tetracycline, and penicillin antibiotics from aqueous solution using activated carbons: Review," *Environ Toxicol Pharmacol*, vol. 50, pp. 1–10, Mar. 2017, doi: 10.1016/j.etap.2017.01.004.

[41] H. Fu *et al.*, "Activated carbon adsorption of quinolone antibiotics in water: Performance, mechanism, and modeling," *Journal of Environmental Sciences*, vol. 56, pp. 145–152, Jun. 2017, doi: 10.1016/j.jes.2016.09.010.

[42] M. N. Alnajrani and O. A. Alsager, "Removal of Antibiotics from Water by Polymer of Intrinsic Microporosity: Isotherms, Kinetics, Thermodynamics, and Adsorption Mechanism," *Sci Rep*, vol. 10, no. 1, p. 794, Jan. 2020, doi: 10.1038/s41598-020-57616-4.

[43] X. Song, D. Liu, G. Zhang, M. Frigon, X. Meng, and K. Li, "Adsorption mechanisms and the effect of oxytetracycline on activated sludge," *Bioresour Technol*, vol. 151, pp. 428–431, Jan. 2014, doi: 10.1016/j.biortech.2013.10.055.

[44] H. Zhou *et al.*, "High capacity adsorption of oxytetracycline by lignin-based carbon with mesoporous structure: Adsorption behavior and mechanism," *Int J Biol Macromol*, vol. 234, p. 123689, Apr. 2023, doi: 10.1016/j.ijbiomac.2023.123689.

[45] C. Yan, L. Fan, Y. Chen, and Y. Xiong, "Effective adsorption of oxytetracycline from aqueous solution by lanthanum modified magnetic humic acid," *Colloids Surf A Physicochem Eng Asp*, vol. 602, p. 125135, Oct. 2020, doi: 10.1016/j.colsurfa.2020.125135.